Differential sensitivity to ionizing radiation in gemcitabine- and paclitaxel-resistant pancreatic cancer cells

Che, P.; Gregori, A.; Bergonzini, C.; Ali, M.; Mantini, G.; Schmidt, T.; ... ; Giovannetti, E.

INTERNATIONAL JOURNAL OF
RADIATION ONCOLOGY • BIOLOGY • PHYSICS
www.redjournal.org

BIOLOGY CONTRIBUTION

Differential Sensitivity to Ionizing Radiation in Gemcitabine-Resistant and Paclitaxel-Resistant Pancreatic Cancer Cells

Pei Pei Che, MSc,[*,†] Alessandro Gregori, MSc,[†,‡,§] Cecilia Bergonzini, MSc,[‖] Mahsoem Ali, BSc,[‡,¶,#] Giulia Mantini, PhD,[†,‡,**] Thomas Schmidt, PhD,[§] Francesco Finamore, PhD,[**] Stephanie M. Fraga Rodrigues, Ing,[†,‡] Adam E. Frampton, MD, PhD,[††] Liam A. McDonnell, PhD,[**] Erik H. Danen, PhD,[‖] Ben J. Slotman, MD, PhD,[*] Peter Sminia, PhD,[*,†] and Elisa Giovannetti, MD, PhD[†,‡,**]

[*]*Department of Radiation Oncology, Amsterdam UMC, Location Vrije Universiteit Amsterdam, Amsterdam, The Netherlands;* [†]*Cancer Biology and Immunology, Cancer Center Amsterdam, Amsterdam, The Netherlands;* [‡]*Department of Medical Oncology, Amsterdam UMC, Location Vrije Universiteit Amsterdam, Amsterdam, The Netherlands;* [§]*Physics of Life Processes, Huygens-Kamerlingh Onnes Laboratory, Leiden University, Leiden, The Netherlands;* [‖]*Leiden Academic Center for Drug Research, Leiden University, Leiden, The Netherlands;* [¶]*Department of Surgery, Amsterdam UMC, Location Vrije Universiteit Amsterdam, Amsterdam, The Netherlands;* [#]*Imaging and Biomarkers, Cancer Center Amsterdam, Amsterdam, The Netherlands;* [**]*Fondazione Pisana per La Scienza, San Giuliano Terme, Italy; and* [††]*Department of Clinical and Experimental Medicine, University of Surrey, Surrey, United Kingdom*

Received Jun 2, 2023; Accepted for publication Oct 22, 2023

Purpose: Chemoresistance remains a major challenge in treating pancreatic ductal adenocarcinoma (PDAC). Although chemoradiation has proven effective in other tumor types, such as head and neck squamous cell carcinoma, its role in PDAC and effect on acquired chemoresistance have yet to be fully explored. In this study, we investigated the sensitivity of gemcitabine-resistant (GR) and paclitaxel-resistant (PR) PDAC cells to ionizing radiation (IR) and their underlying mechanisms.

Methods and Materials: GR and PR clones were generated from PANC-1, PATU-T, and SUIT2-007 pancreatic cancer cell lines. Cell survival after radiation was assessed using clonogenic assay, sulforhodamine B assay, apoptosis, and spheroid growth by bioluminescence. Radiation-induced DNA damage was assessed using Western blot, extra-long polymerase chain reaction, reactive oxygen species production, and immunofluorescence. Autophagy and modulation of the Hippo signaling pathway were investigated using proteomics, Western blot, immunofluorescence, and reverse-transcription quantitative polymerase chain reaction.

Results: In both 2- and 3-dimensional settings, PR cells were more sensitive to IR and showed decreased β-globin amplification, indicating more DNA damage accumulation compared with GR or wild-type cells after 24 hours. Proteomic analysis of PR PATU-T cells revealed that the protein MST4, a kinase involved in autophagy and the Hippo signaling pathway, was highly downregulated. A differential association was found between autophagy and radiation treatment depending on the cell model.

Corresponding author: Elisa Giovannetti, MD, PhD; E-mail: e.giovannetti@amsterdamumc.nl

Pei Pei Che and Alessandro Gregori made equal contributions to this study.

Peter Sminia and Elisa Giovannetti made equal contributions to this study.

Disclosures: The authors declare no conflict of interest. This study was supported by Zabawas Foundation (Grant #CCA 2019-5-55), Living with Hope Foundation (personal grant to P.P.C.), KWF Dutch Cancer Society (Grant Number 11957), and Associazione Italiana per la Ricerca sul Cancro (AIRC/IG-grant number 24444).

Data Sharing Statement: Research data are stored in an institutional repository and will be shared upon request to the corresponding author.

Acknowledgments—The authors thank Simon Tóth for his assistance, Prof Dr Arjan Griffioen and his team for use of the automated microscope station, and Ida van der Meulen-Muileman for provision of antibodies and reagents.

Supplementary material associated with this article can be found in the online version at doi:10.1016/j.ijrobp.2023.10.035.

Int J Radiation Oncol Biol Phys, Vol. 118, No. 5, pp. 1328–1343, 2024
0360-3016/$ - see front matter
https://doi.org/10.1016/j.ijrobp.2023.10.035

Interestingly, increased yes-associated protein nuclear localization and downstream Hippo signaling pathway target gene expression were observed in response to IR.

Conclusions: This was the first study investigating the potential of IR in targeting PDAC cells with acquired chemoresistance. Our results demonstrate that PR cells exhibit enhanced sensitivity to IR due to greater accumulation of DNA damage. Additionally, depending on the specific cellular context, radiation-induced modulation of autophagy and the Hippo signaling pathway emerged as potential underlying mechanisms, findings with potential to inform personalized treatment strategies for patients with acquired chemoresistance.

Introduction

The development of chemoresistance is a major challenge in the treatment of pancreatic ductal adenocarcinoma (PDAC), which accounts for the majority of pancreatic cancer cases. With as many diagnosed patients as deaths and a low 5-year overall survival (OS) rate of 12%, PDAC has a prognosis that remains one of the poorest compared with other solid tumor types.[1,2] Surgical resection is only possible for a small percentage of patients (15%-20%), leaving the majority to rely on chemotherapy as the primary treatment option.[3] Gemcitabine in combination with nab-paclitaxel and the combination of 5-fluorouracil, leucovorin, irinotecan, and oxaliplatin (FOLFIRINOX) are the most widely used chemotherapy regimens for treatment of locally advanced PDAC.[4] Despite the use of such polychemotherapeutic regimens, patients eventually develop progressive disease, indicative of therapy resistance, highlighting that chemoresistance remains a major limitation in PDAC treatment and underlining the urgent need to develop therapeutic strategies to overcome this obstacle.

Although approximately 50% of solid tumor types are treated with or in combination with ionizing radiation (IR), radiation therapy (RT) is not regularly included within the repertoire of PDAC treatments in Europe. With advancements in RT through improved delivery techniques and emergence of types of particle radiation, such as proton radiation, clinical trials are being conducted to evaluate different combination approaches at different disease stages (eg, resectable and locally advanced).[5] The recent long-term results of the Dutch PREOPANC-1 trial showed that neoadjuvant chemoradiation with gemcitabine for patients with borderline resectable PDAC resulted in a 3-fold increase in 5-year OS compared with upfront surgery followed by adjuvant gemcitabine.[6] Thus, the addition of radiation could be a feasible treatment approach, although it is uncertain whether acquired resistance to chemotherapy could affect the response to IR.

In terms of mechanism, RT arrests tumor growth and clonogenic capacity by inducing DNA damage in aberrantly proliferating cancer cells.[7] Although RT is ideally applicable to all tumor types, radiation sensitivity is variable among neoplastic malignancies. This is mainly due to alterations in pathways that allow evasion of DNA damage−induced cell death, thereby reducing the therapeutic effectiveness of radiation.[8] Autophagy and Hippo signaling have been identified among the various altered pathways involved in differential sensitivity to radiation.[8-10]

Macroautophagy has long been studied as a mechanism that cancer cells employ to evade cell death induced by stressors, such as radiation.[11] Hippo signaling regulates cell proliferation and apoptosis and is an emerging interesting target for both PDAC and modulation of radiation response.[9,12] Interestingly, expression of the downstream transcription factor yes-associated protein (YAP) and nuclear translocation were reported to be affected by IR and to modulate radiosensitivity in some cancer types.[13,14] However, determination of whether these mechanisms are also involved in differential response to IR in PDAC and whether chemoresistant cells have altered autophagy or Hippo signaling remains elusive. Therefore, to determine whether there is differential radiosensitivity upon acquired chemoresistance, we examined 3 human PDAC cell lines with previously generated gemcitabine-resistant (GR) and paclitaxel-resistant (PR) clones. This study initially assessed the sensitivity of the GR and PR clones to −IR compared with their parental cells, as well as the differences in radiosensitivity between the different clones. Remarkably, PR cells demonstrated greater sensitivity to IR than both parental and GR cells in both 2-dimensional (2D) and 3-dimensional (3D) models. This sensitivity was associated with an accumulation of DNA damage in PR cells. As putative mechanisms underlying the increased radiosensitivity, autophagy and the Hippo signaling pathway were investigated.

Methods and Materials

Cell culture

The PDAC PATU-T cell line was kindly gifted by Dr. Irma van Die (Amsterdam UMC, Amsterdam, The Netherlands), the SUIT2-007 cell line by Dr. Adam E. Frampton, and the GR PANC-1 cell line by the Institute for Surgical Research, Philips-University of Marburg. The PANC-1 cell line was purchased from ATCC. All cell lines were kept in culture at 37 °C and 5% CO_2. The PANC-1 and SUIT2-007 cells were cultured in RPMI-1640 medium (Gibco) and the PATU-T cells in High-Glucose Dulbecco's Modified Eagle Medium (Gibco). All cells were supplemented with 10% heat-inactivated new-born calf serum (Biowest) and 1% penicillin/streptomycin (Lonza). Cells were tested for mycoplasma by polymerase chain reaction (PCR) via Eurofins Genomics. All PATU-T and SUIT2-007 cell lines were lentivirally transduced with pUltra-Chili-Luc (Addgene, Plasmid

#48688), stably expressing firefly luciferase (FLuc) and dTomato, using a methodology previously described.[15]

Generation of GR and PR clones

Chemoresistant cell lines were generated and characterized as previously described[16] and as shown in Figure E1. In brief, cells were continuously exposed to the drug with a stepwise increasing concentration until the maximum tolerated dose was reached. For all experiments, cells without drug treatment for at least 2 consecutive passages were used.

Radiation treatment

Cells and spheroids were irradiated at room temperature with the indicated X-ray doses using the CellRad Benchtop X-ray Irradiator (Precision X-ray) at a dose rate between 0.8 and 1.2 Gy/min.

Colony formation assay

Colony formation assays were performed as described.[17] Briefly, cells were seeded at a low cell density (250-10,000 cells per well) in 6-well plates (VWR) to form colonies in normal culturing conditions. After 10 to 14 days, colonies were washed with sterile phosphate-buffered saline (PBS), fixated in absolute ethanol for 15 minutes, and stained with 0.5% weight/volume crystal violet in deionized water for 30 minutes at room temperature. Next, plates were washed 5 times in deionized water and left to dry overnight. Plates were scanned and analyzed using the GelCount Tumour Colony Counter (Oxford Optronix). Only clones with >50 cells were included. Plating efficiency (PE) and cell survival fractions (SF) were calculated using the formulas

$$PE = \frac{Number\ of\ colonies}{Number\ of\ cells\ seeded}$$

$$SF = \frac{PE\ (treatment)}{PE\ (untreated)}$$

Cell viability and cell death assays

Cell viability and cell death was assessed by sulforhodamine B (SRB) assay and apoptosis assay, respectively, as described.[18,19] For both assays, cells were seeded in 96-well plates at a density of 3000 to 4000 cells per well and irradiated 24 hours after seeding. Cells were fixated in 50% weight/volume trichloroacetic acid (TCA) 72 hours post-RT and stained with SRB solution, and the absorbance was read at 490 nm with a BioTek Synergy HT Spectrophotometer (Agilent). For the apoptosis assay, cells were washed with PBS 72 hours post-RT, stained with fluorescein isothiocyante (FITC) using FITC Annexin V (VPS Diagnostics, Cat. #A705) and propidium iodide (Cat. #P4170) in the provided binding buffer and fluorescence (FITC, excitation = 485 nm and emission = 535 nm; propidium iodide, excitation = 536 nm and emission = 617 nm) was measured with a BioTek Plate Reader. After fluorescence measurement, cells were fixated with TCA and stained with SRB as described previously. Finally, fluorescence intensity was corrected by the number of cells per well.

Spheroid formation assay

Spheroids were generated by seeding 3500 cells per well in 96-Well PS U-Bottom Clear Microplates (Greiner BioOne, #650970) using the method described by Ware et al.[20] Cells were seeded in a final concentration of 0.24% weight/volume methylcellulose in supplemented High-Glucose Dulbecco's Modified Eagle Medium or RPMI-1640 medium. After 24 hours of incubation, spheroids were irradiated with 4 Gy and left to incubate for 7 to 10 days in standard culturing conditions. The medium was refreshed twice a week with fresh 0.24% weight/volume methylcellulose in medium. Images were taken with a Leica DM3000 B Microscope (Leica Microsystems) at a magnification of 5 × . Spheroid growth was calculated by measuring Feret's diameter with Fiji software.

Bioluminescence assay

FLuc activity was determined as a measure of cell viability as adjusted and described.[21-23] Briefly, adherent cells or spheroids were lysed in FLuc Assay Reagent (final concentrations of 20 mM Tris-HCl, 1% Triton X-100, 10 mM of $MgCl_2$, 250 μM of $Na_2H_2P_2O_7$, and 2 mM of dithiothreitol at pH of 7.8) and gently shaken on a plate shaker for 10 minutes at room temperature. Samples were transferred to opaque Greiner Bio-One Lumitrac 200 96-Well Microplates (Greiner Bio-One, #655075) and the substrate solution added (final concentrations of 100 μM D-luciferin and 250 μM adenosine triphosphate in FLuc Assay Reagent). PANC-1 spheroids were transferred to Lumitrac 200 plates and cell viability was measured using CellTiter-Glo Cell Viability Assay in a 1:1 ratio according to the manufacturer's protocol (Promega, #G755B). BLI was measured immediately using the BioTek Plate Reader with 1 second of reading per sample. Linear regression models for both spheroids and cells grown as monolayers were analyzed in R version 4.0.3.

Western blot

Forty micrograms of proteins per sample were loaded on sodium dodecyl sulfate–polyacrylamide gels and transferred to polyvinylidene difluoride membranes. Membranes were visualized with Amersham ECL Western Blotting Detection Kit (GE HealthCare, RPN2232). Additional information and details regarding the antibodies are described in

Appendix E1. All uncut, original membranes used in the figures are shown in Figures E2 to E4.

Reactive oxygen species assay

Generation of reactive oxygen species (ROS) upon radiation was assessed as described.[24] Cells were seeded in a 96-well plate at a cell density of 15,000 cells per well. Cells were washed with PBS 24 hours after seeding and incubated with 10 μM of 2′,7′-dichlorofluorescin diacetate solution (Sigma-Aldrich, #D6883) for 45 minutes at 37 °C and 5.0% CO_2. After washing off the diacetate solution, cells were irradiated and relative fluorescence in units was measured after 30 minutes using the BioTek Plate Reader with a fluorescence excitation of 485 nm and fluorescence emission of 535 nm. Lastly, cells were fixated with 50% weight/volume TCA followed by SRB staining as described previously. Fluorescence intensity was corrected by the number of cells per well.

Quantitative PCR

RNA was extracted from adherent cells 72 hours post-RT using TriZol Reagent (Invitrogen) according to the manufacturer's instructions. Untreated samples were collected simultaneously with the 72-hour post-RT samples. A total of 0.5 μm of RNA was used to retrotranscribe cDNA with the First Strand cDNA Synthesis Kit (Thermo Scientific, #K1612) according to the manufacturer instructions. Reverse-transcription quantitative PCR was conducted with SsoAdvanced Universal SYBR Green Supermix (Bio-Rad, #172-5271) in a CFX96 Real-Time System (Bio-Rad) apparatus. Primer sequences (Invitrogen) for connective growth factor (CTGF) and beta-actin (β-actin) were as follows: CTGF (forward): CCAATGACAACGCCTCCTG; CTGF (reverse): TGGTGCAGCCAGAAAGCTC; β-actin (forward): GCGAGAAGATGACCCAGAT; β-actin (reverse): GAGGCGTACAGGGATAGC. Relative mRNA expression was calculated with the $2^{-(\Delta\Delta Ct)}$ method.

Extra-long PCR

DNA was extracted from adherent cells 24 hours post-RT using TriZol Reagent and extra-long PCR was performed as described[17] to assess accumulated DNA damage in an extended region of primers.

Immunofluorescence

To examine YAP subcellular localization, cells were seeded on cover glass at a density of 1×10^5 cells per well and irradiated the following day with 4 Gy. Cells were fixated 72 hours post-RT with 4% paraformaldehyde for 15 minutes, permeabilized with 1% Triton-X 100 for 10 minutes, blocked in 5% weight/volume bovine serum albumin, and incubated for 1 hour with primary antibody followed by 1 hour of incubation with secondary antibody. Cells were visualized with a Nikon Eclipse Ti2 Confocal Microscope and 100 × oil objective. Nucleus-to-cytosol ratio was calculated with MATLAB software.

Spheroids were generated as previously described. At 7 days post-RT, spheroids were fixated in 4% paraformaldehyde overnight at 4 °C, permeabilized 1 hour at room temperature with 1% Triton X-100, blocked 1 hour with 5% weight/volume of bovine serum albumin, and incubated overnight at 4 °C with primary antibody followed by 2 hours of incubation with secondary antibody. Whole spheroids were then imaged with an Axiovert200 Confocal Microscope, coupled to a Yokogawa Spinning Disk unit and an EMCCD Camera using a 10 × air objective. A Z-stack of 40.8 μm with a step of 2.4 μm was acquired for each sample, and images were processed with Fiji software. All information regarding antibodies is described in Appendix E1.

Statistical analysis

Statistical analyses were performed using GraphPad Prism version 9.0. All statistical analyses were performed using multiple Mann-Whitney *t* tests to determine YAP nucleus-to-cytoplasm ratios and CTGF levels or unpaired Student *t* tests for comparisons of the survival fractions. Comparisons of β-globin amplifications, cell viability, and apoptotic fractions were performed using 2-way analysis of variance with Tukey's multiple comparisons test. Comparisons of spheroid data between untreated and irradiated groups were performed using proportional odds ordinal logistic regression modeling with treatment-by-cell line interaction. Continuous outcomes were analyzed with proportional odds ordinal logistic regression models. Differences in treatment effect between cell lines were assessed with treatment-cell line interactions and with likelihood ratio tests for the treatment-cell line interaction term. $P < .05$ was considered statistically significant.

Results

PR PDAC cells demonstrate increased radiosensitivity in 2D models

PDAC cell lines PANC-1, PATU-T, and SUIT2-007 were successfully used to generate GR and PR clones, as previously described[16] and as shown in Figure E1. PATU-T and SUIT2-007 were chosen to represent a highly mesenchymal phenotype and PANC-1 as an intermediate (epithelial/quasi-mesenchymal) phenotype. Given the aggressiveness and late diagnosis of PDAC, all the experiments were performed on the mesenchymal cell lines PATU-T and SUIT2-007 and repeated for validation endpoint by quantitative assays with the quasi-mesenchymal cell line PANC-1. To determine their sensitivity to IR and clonogenic capacity, cells were seeded for colony formation assays and treated with increasing radiation doses. Although the resulting

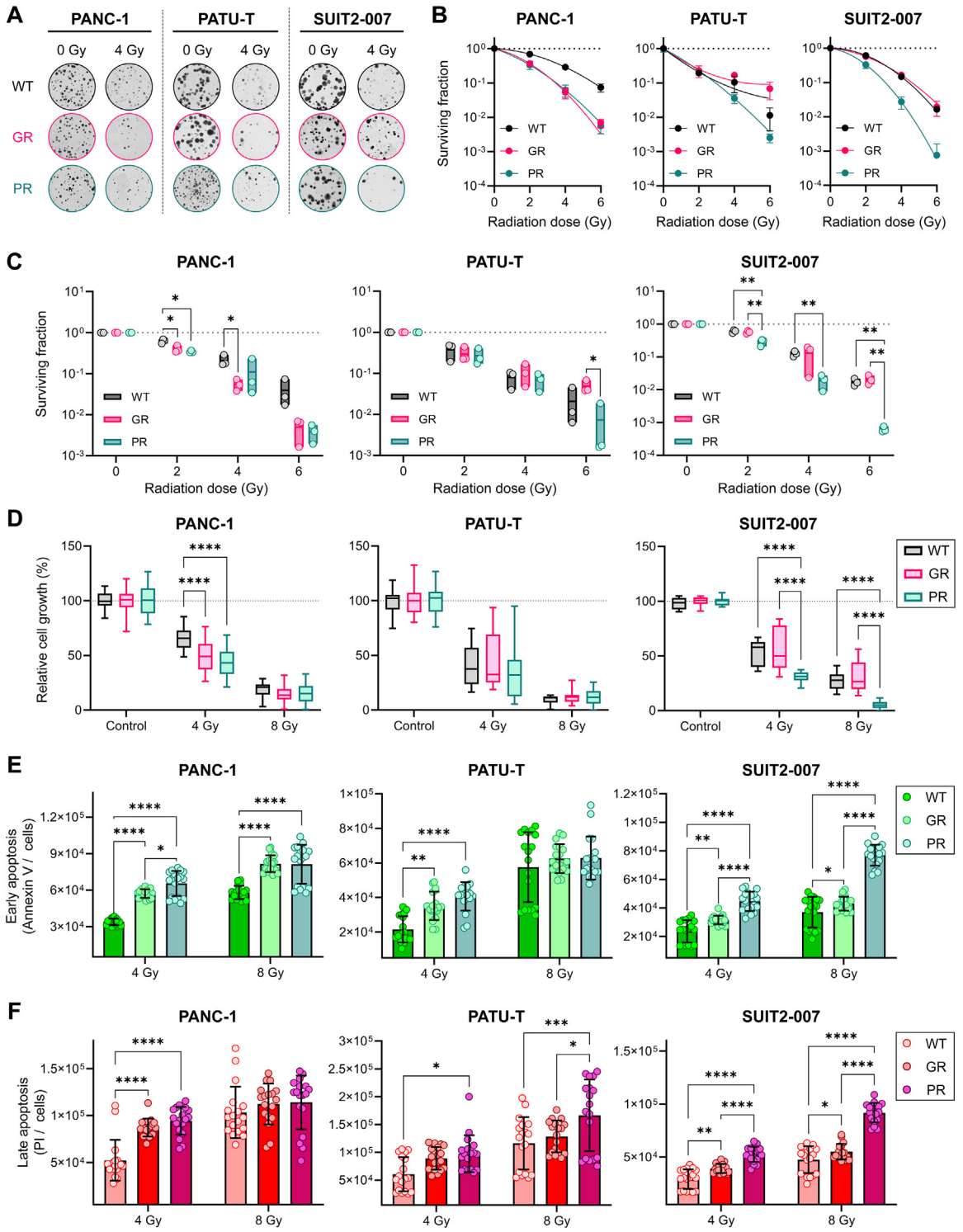

Fig. 1. Paclitaxel-resistant human pancreatic ductal adenocarcinoma cell lines are sensitive to radiation. (A) Representative images of colonies and (B) representative cell survival curves from an individual experiment evaluating wild-type PANC-1, PATU-T, and SUIT2-007 cells and derived gemcitabine-resistant and paclitaxel-resistant clones obtained from colony formation assays. (C) Survival fractions after increasing radiation doses. Data represent the means of 3 individual experiments ± SEM. (D) Cell growth percentage relative to untreated controls of irradiated cells at the indicated dose as assessed by sulforhodamine B assay. Data are represented by boxplots showing the minimum to maximum and a line at the median of 3 individual experiments. Induction of (E) early and (F) late apoptosis after irradiation as assessed by fluorescein isothiocyanate staining using FITC Annexin V and propidium iodide staining, respectively. Data are expressed as means of Annexin V or propidium iodide fluorescent intensity corrected for the number of cells ± SEM of 3 individual experiments. *P* values for cell growth and apoptosis are presented as $^{*}P < .05$, $^{**}P < .01$, $^{***}P < .001$, $^{****}P < .0001$. *Abbreviations:* GR = gemcitabine resistant; PI = propidium iodide; PR = paclitaxel resistant; WT = wild type.

colonies from both the GR and PR clones appeared similar to the parental cells from which they were derived (Fig. 1A), we observed distinctive differences in the cell survival curves among the wild-type (WT), GR, and PR clones derived from all 3 commercial cell lines (Fig. 1B). In particular, PR clones demonstrated a decreasing survival fraction starting at 2 Gy in PANC-1 and SUIT2-007 cells, whereas a trend toward differential response was observed in PR PATU-T cells from 4 Gy (Fig. 1B, C). Conversely, GR clones for both PATU-T and SUIT2-007 cells demonstrated almost similar radiosensitivity, which was comparable to their parental cells (Fig. 1B). PANC-1 cells were the exception, as both chemoresistant (GR and PR) clones displayed increased sensitivity to IR compared with parental PANC-1 cells.

To further investigate the differential sensitivity of chemoresistant cells to IR, cell growth inhibition and apoptosis induction were assessed. The doses selected were 4 Gy, at which differential response was first observed, and 8 Gy, a sublethal dose for all our cell lines. Interestingly, a dose-dependent cell growth decrease was observed. At 4 Gy, irradiation reduced cell proliferation in all cell lines by ~50%, with PR PANC-1 and PR SUIT2-007 clones being more radiosensitive than their WT clones (Fig. 1D). At 8 Gy, all cell lines showed growth inhibition of 80% except for WT and GR SUIT2-007 clones, which were more resistant to IR compared with the PR clone (Fig. 1D). Consistently, apoptosis induction after 4 Gy showed a similar trend, with increased early and late apoptosis in PR cells compared with GR or WT cells (Fig. 1E, F). At 8 Gy, we observed a cell line differential response to either early or late apoptosis, but with PR cells as the most sensitive in all cases (Fig. 1E, F). Collectively, these results indicate that PR PDAC cells are more sensitive to IR as proven by decreased clonogenic cell survival, reduced cell proliferation, and enhanced induction of apoptosis.

PR PDAC cells demonstrate increased radiosensitivity in 3D models

As previous studies demonstrated that 3D tumor models are more suitable for mimicking the clinical situation,[23,25] we employed spheroid models to further validate the observed differential radiosensitivity among our chemoresistant models. Spheroids were irradiated with 4 Gy and the diameter was measured daily for 10 days after radiation. By measuring the spheroid diameter, a radiation-induced growth delay was observed over time with the exception of WT and PR PANC-1 cells and GR PATU-T cells, which could be attributed to their slow spheroid growth (Fig. 2A). To quantify the effect of radiation on the cell viability of 3D spheroids, an established method based on luciferase assay was employed.[23] PATU-T and SUIT2-007 cells and their chemoresistant counterparts were lentivirally transduced to stably express FLuc and dTomato. The transduction efficiency was first evaluated in 2D by both immunofluorescence (Fig. 2B) and BLI by correlating the number of seeded cells in terms of increased relative light units (RLUs) (Fig. 2C). However, in 3D spheroids, we observed that the number of cells seeded initially do not linearly correlate to the RLU number (Fig. E5A). To validate that the number of RLUs produced is proportional to the number of viable cells in spheroids, we examined the correlation between the spheroid diameter and the RLU number produced. Our analysis confirmed that larger spheroids containing a greater number of viable cells and increased diameter produced a higher BLI signal (Fig. 2D). Furthermore, when we assessed the spheroid growth 7 days post-RT, we observed a significant decrease in BLI and diameter when compared with treatment effect between PR PATU-T and GR PATU-T cells ($P = .016$) and for PR SUIT2-007 vs. WT SUIT2-007 cells ($P = .001$) and GR SUIT2-007 cells ($P = .004$) (Figs. 2E and E5B).

PANC-1 spheroids, especially WT and PR PANC-1 spheroids, showed a slow growth rate for both treatment conditions, as reflected by the small increase in diameter from day 1 to 8 (Fig. 2A). This slow growth could partially explain the lack of an observable decrease in BLI nor diameter between 0 and 4 Gy for both WT and PR PANC-1 cells. On the other hand, GR PANC-1 cells demonstrated a significant decrease in BLI that was also reflected by the decrease in diameter after radiation, which could be attributed to their faster growth rate as spheroids. Interestingly, after 10 days post-RT, the difference in radiation-induced spheroid growth delay was less pronounced, which is attributed to compensation for the delay by cell proliferation (Fig. E5C). These results provide further evidence that the mesenchymal cell lines PATU-T and SUIT2-007 with acquired paclitaxel resistance demonstrate increased radiosensitivity.

Radiation-induced DNA damage and ROS production are increased in PR PDAC cells

DNA is the critical target for radiation-induced cell death.[7] We employed phosphorylated histone 2AX (γH2AX) as a marker to assess the initiation and recovery of DNA double-stranded breaks (DSBs). This analysis revealed enhanced γH2AX expression, particularly at the outer regions of the irradiated spheroids, compared with untreated spheroids (Fig. 3A). Interestingly, basal γH2AX expression was increased in both untreated PR PATU-T and PR SUIT2-007 spheroids. To explore the potential impairment of DNA damage repair, we conducted Western blot analysis to examine the protein expression of γH2AX. After 30 minutes of radiation, we observed a significant upregulation of γH2AX that subsequently returned to baseline levels at 24 hours in both cell lines, irrespective of their chemoresistant status (Fig. 3B).

To quantitatively evaluate the extent of accumulated DNA damage, we employed extra-long PCR using a long-range PCR fragment, a technique used to assess the effect of other DNA-damaging modalities, such as cisplatin.[26] Intriguingly, PR clones of all 3 PDAC cell lines exhibited a

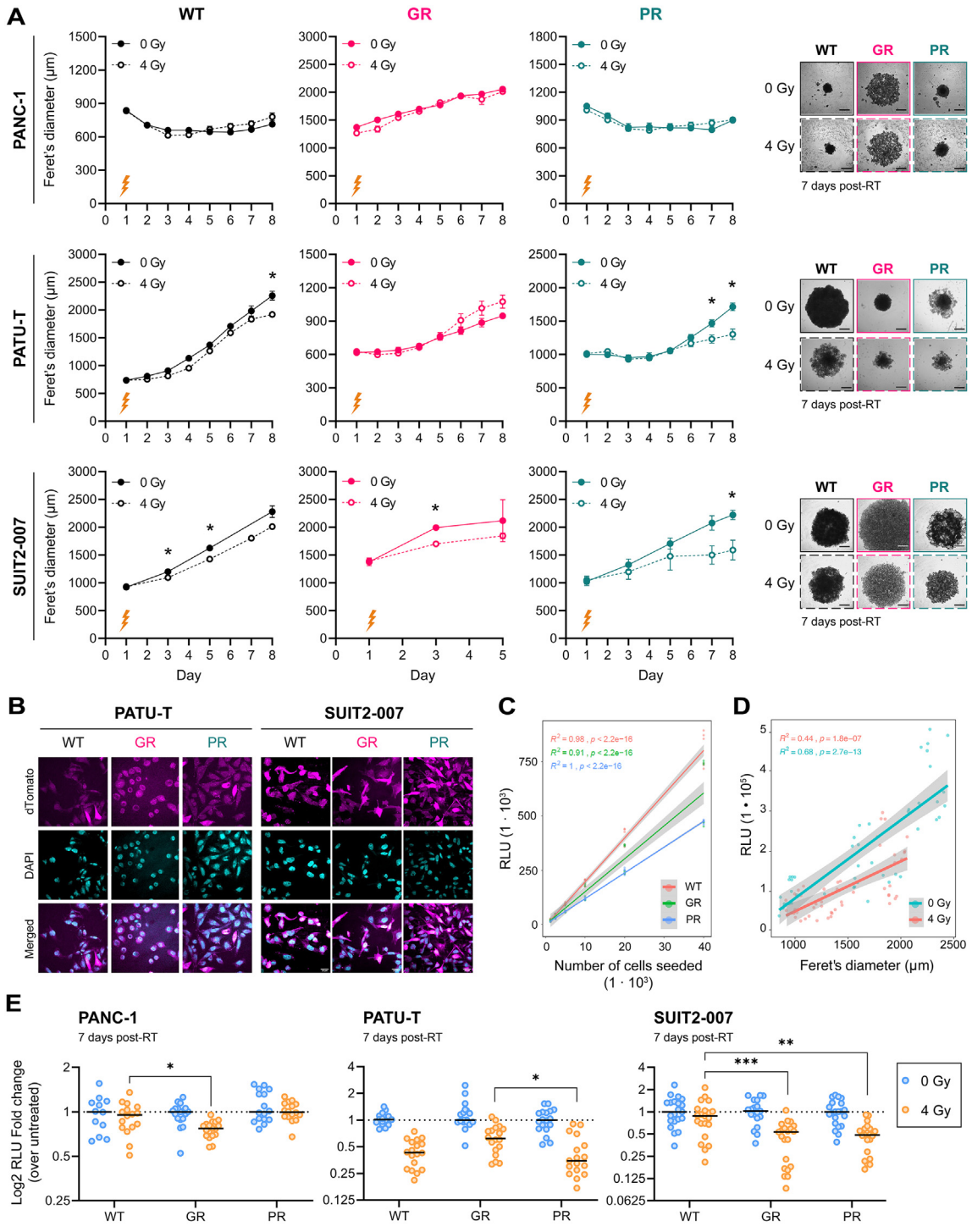

Fig. 2. Increased radiosensitivity in paclitaxel-resistant pancreatic ductal adenocarcinoma spheroids. (A) Spheroids of PANC-1 (top panel), PATU-T (middle panel), and SUIT2-007 (bottom panel) were irradiated with 4 Gy 24 hours after seeding and the diameter measured daily for 10 days after radiation. The Feret's diameter was used as a measure for the size of the spheroid; the curves were truncated when no data points were available due to the spheroids outgrowing the field of view. Representative brightfield images of untreated and irradiated spheroids are shown 7 days after radiation (right panels). Scale bar = 500 μm. (B) Transduction efficiency was inspected using dTomato expression and DAPI staining for the nucleus of the cell. Linear correlation was performed of (C) cell number against RLUs from PATU-T cells and (D) Feret's diameter against RLUs from untreated and irradiated PATU-T spheroids. (E) Cell viability of PANC-1, PATU-T, and SUIT2-007 spheroids 7 days after radiation was measured via bioluminescence assay. Medians are shown as black lines. Data represent the means of 3 individual experiments ± SEM. $^{*}P < .05$, $^{**}P < .01$, $^{***}P < .001$. *Abbreviations:* GR = gemcitabine resistant; PR = paclitaxel resistant; RLU = relative light unit; RT = radiation therapy; WT = wild type.

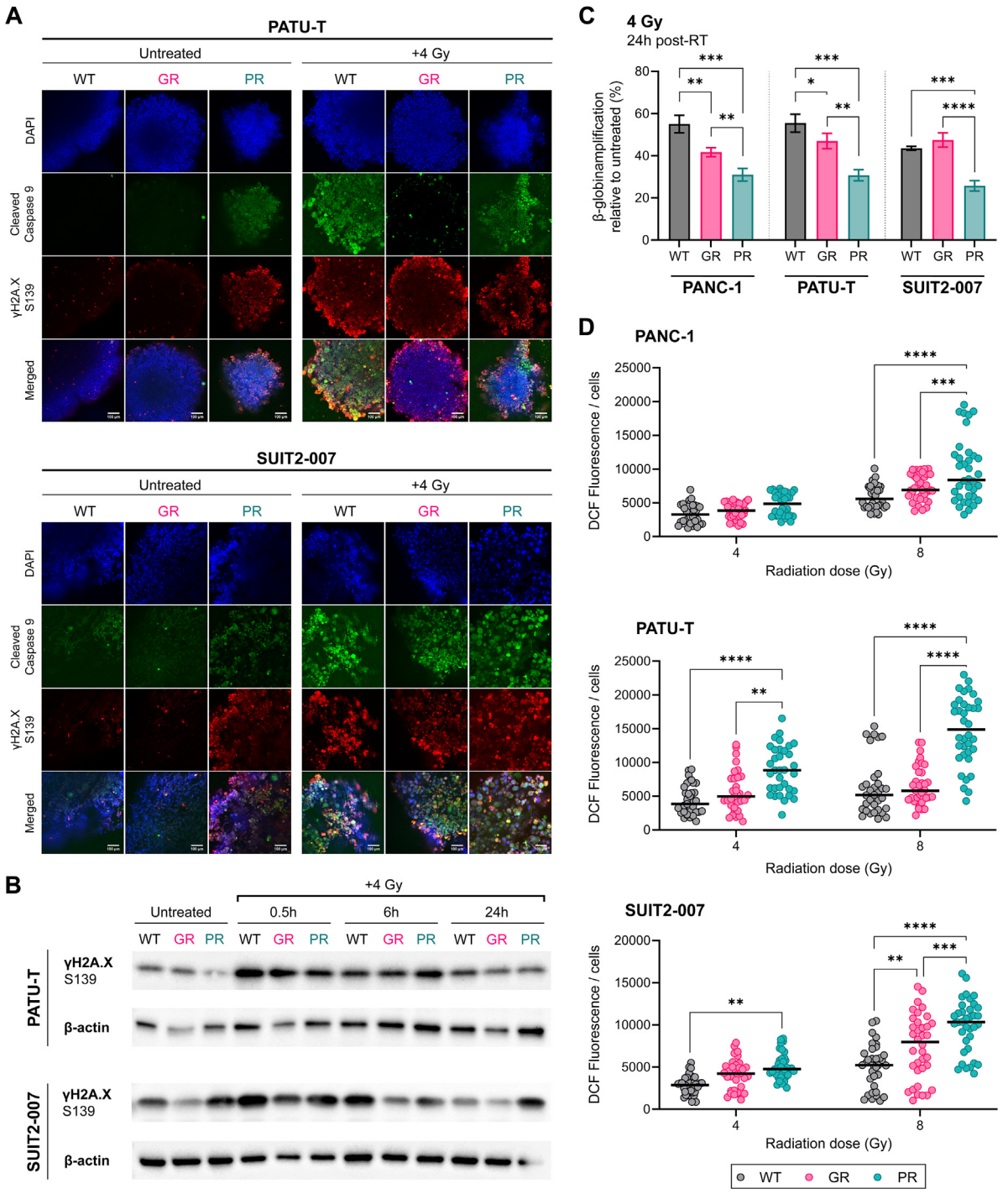

Fig. 3. Radiation-induced DNA damage is increased in paclitaxel-resistant cells. (A) Representative confocal images of untreated and irradiated spheroids stained with DNA double-strand break marker γH2AX (S139; red), cleaved caspase 9 (green), and DAPI for the nucleus (blue). Scale bar = 100 μm. (B) Protein expression of γH2AX (S139) after 4 Gy of radiation was investigated at 0.5, 6 and 24 hours after radiation for PATU-T and SUIT2-007 cells using Western blot. (C) Beta-globin amplification as a measure of accumulated DNA damage was determined after 4 Gy of radiation. Data represent the means ± SD from 2 individual experiments. (D) Generation of reactive oxygen species was measured after 4 and 8 Gy of radiation using dichlorofluorescein fluorescent intensity assay corrected for the number of cells. Data points are shown from 3 individual experiments and the medians are represented by black lines. *$P < .05$, **$P < .01$, ***$P < .001$, ****$P < .0001$. *Abbreviations:* DCF = dichlorofluorescein; GR = gemcitabine resistant; PR = paclitaxel resistant; RT = radiation therapy; WT = wild type.

notable increase in accumulated DNA damage post-RT, as evidenced by the reduction in β-globin amplification (Fig. 3C). Interestingly, GR clones from PANC-1 and PATU-T cells showed more DNA damage accumulation compared with WT clones but not to the level of PR clones, although no difference was observed between SUIT2-007 WT and GR clones.

In addition to direct damage to the DNA, IR could affect the cell indirectly, in particular through radiolysis of water and increased ROS production, eventually causing indirect DNA damage.[7] Because we observed elevated DNA damage accumulation in PR clones, we further investigated whether IR induces an increase in ROS generation in PR clones. In all 3 cell lines, PR clones consistently demonstrated elevated ROS production compared with their derived parental cells, evidenced by increased dichlorodihydrofluorescein fluorescence at both 4 and 8 Gy for both PATU-T and SUIT2-007 cells (Fig. 3D). For PR PANC-1 cells this differential increase in ROS production was only significant at 8 Gy.

Proteomics and expression of MST4

To investigate the molecular mechanism underlying the increased radiosensitivity observed in PR PDAC cells, we reanalyzed previously recorded proteomics data.[16] We hypothesized that this enhanced response to IR could be attributed to the loss or extensive downregulation of specific proteins present in the WT cells. Consequently, we focused on the top 20 proteins that were exclusively present in the parental cells but below the detection threshold in the PR cells (Table 1). Using the results, we performed a literature

Table 1 Comparison of top 20 downregulated proteins in PR and WT PATU-T cells

		Log_2 transformed protein abundances						
Gene ID	Protein name	WT	WT	WT	PR	PR	PR	Radiosensitivity/resistance
STK26/MST4	Serine/threonine-protein kinase 26	23.39	23.39	24.25	-	-	-	Radioresistance GBM
CUTA	CutA divalent cation tolerance homolog	23.00	23.05	23.52	-	-	-	NA
NDUFA3	NADH:ubiquinone Oxidoreductase subunit A3	22.07	22.90	23.93	-	-	-	NA
NME4	Nucleoside diphosphate kinase 4	22.42	22.90	22.80	-	-	-	NA
SPCS1	Signal peptidase complex subunit 1	23.84	21.36	22.47	-	-	-	NA
SLC4A7	Sodium bicarbonate cotransporter 3	22.19	22.61	22.78	-	-	-	NA
ASAP2	ArfGAP with SH3 domain	22.04	23.21	22.07	-	-	-	NA
CYP24A1	Cytochrome P450 family 24	21.07	23.52	22.72	-	-	-	NA
HAGH	Hydroxyacylglutathione Hydrolase	22.91	22.13	21.65	-	-	-	NA
MAP1B	Microtubule-associated protein 1B	22.97	22.47	21.25	-	-	-	NA
TEX30	Testis-expressed protein 30	22.36	23.25	20.61	-	-	-	NA
PLEKHH1	Pleckstrin homology domain-containing family H member 1	21.56	22.61	22.00	-	-	-	NA
GPN1	GPN-loop GTPase 1	23.10	20.42	22.61	-	-	-	NA
TP53I3	Tumor protein P53 inducible protein 3	22.36	21.61	21.61	-	-	-	Radioresistance GBM
RANBP9	RAN binding protein 9	21.61	21.36	22.31	-	-	-	NA
GCDH	Glutaryl-CoA dehydrogenase	21.13	22.39	21.56	-	-	-	NA
MAPRE2	Microtubule-associated protein RP/EB family member 2	21.90	20.70	22.34	-	-	-	NA
FMNL2	Formin-like protein 2	20.42	21.93	22.54	-	-	-	Radiosensitivity Nasopharyngeal carcinoma
PMF1	Polyamine-modulated factor 1	23.15	21.82	19.46	-	-	-	NA
TMEM256	Transmembrane protein 256	20.86	23.25	20.07	-	-	-	NA

Proteins are listed from highest to lowest protein abundance observed in WT cells filtered against PR cells that consistently displayed no observable intensities. Protein abundance of WT cells is listed as the log_2 transformed data value from 3 replicates assessed for known association with radiosensitivity or resistance in the literature.

Abbreviations: GBM = glioblastoma; NA = not applicable; PR = paclitaxel resistant; WT = wild type.

search to explore any potential connections with radiation responsiveness.

Our analysis identified serine threonine kinase 26 (STK26) as the top hit among the downregulated proteins in PR PATU cells (Table 1). STK26 or mammalian STE20-like protein kinase (MST4) is a serine/threonine kinase known to confer radioresistance in glioblastoma through the regulation of the autophagy pathway.[27] To validate the downregulation of MST4, we performed Western blot analysis, which confirmed its decreased expression in PR PANC-1 and PATU-T cells. However, PR SUIT2-007 cells did not exhibit the same pattern (Fig. 4A). Based on these findings, we were prompted to further investigate various downstream pathways associated with MST4, including autophagy and modulation of the Hippo pathway.

Radiation-induced autophagy is cell-line dependent

Autophagy has been widely investigated as a mechanism of protection against stressors, such as radiation.[11] Of note, autophagy can play a multifaceted role in the response of cancer cells to RT, either through the promotion of cell survival and DNA repair or radiation-induced cell death via excessive self-digestion with cellular senescence or apoptosis as a consequence.[28,29] Therefore, we investigated whether our PR cells had impaired autophagic activity compared with their WT and GR clones by examining the modulation of bona fide autophagosome markers p62 and LC3B. More precisely, we investigated the increase in LC3 II/I ratio and p62 degradation, which are indicators of autophagy activation because autophagosomes are fused with lysosomes to

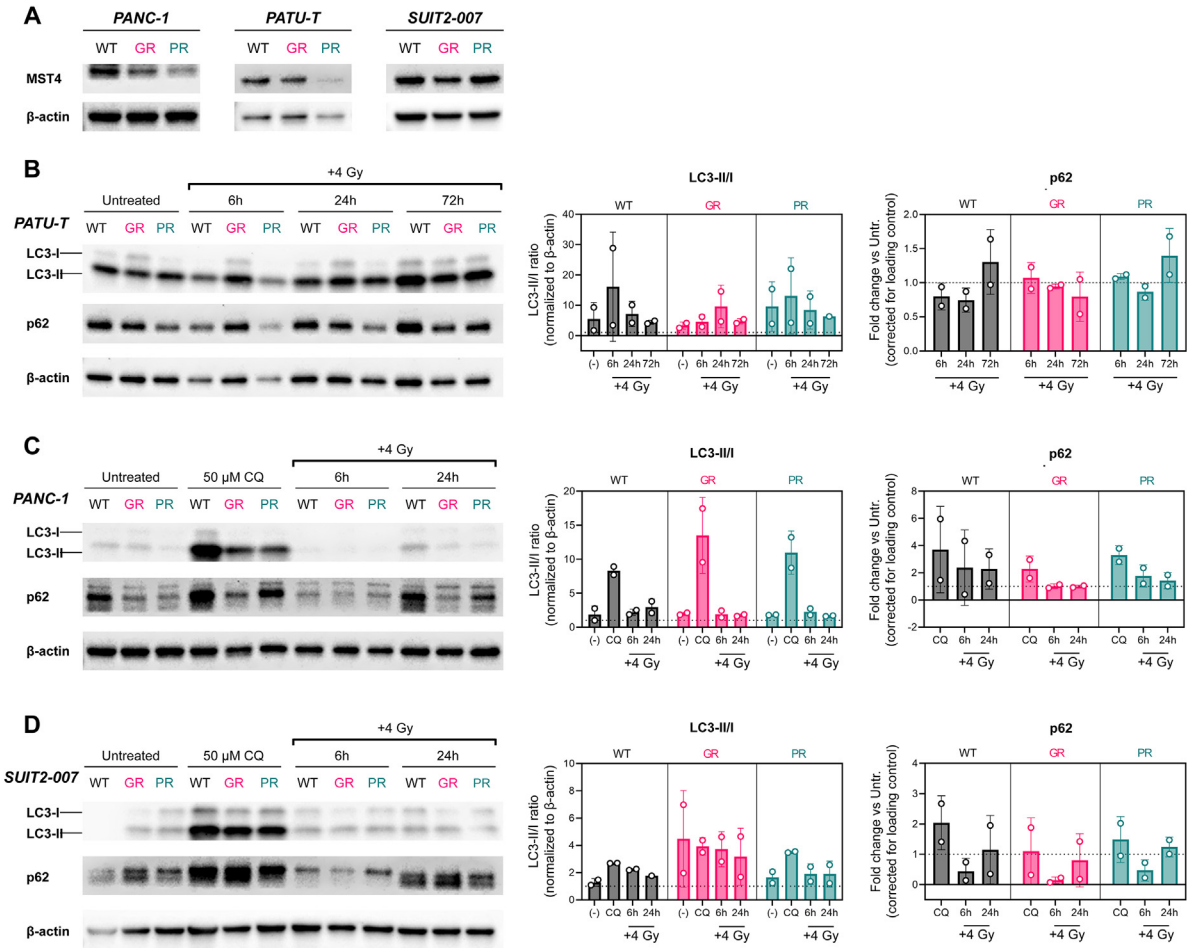

Fig. 4. Radiation-induced autophagy is cell-line dependent. (A) Protein expression of MST4 in PANC-1, PATU-T, and SUIT2-007 cells was determined using Western blot. Downstream autophagy markers, including LC3B and their corresponding isoforms I and II and p62, were investigated using Western blot in (B) PATU-T, (C) PANC-1, and (D) SUIT2-007 cells. Quantification of LC3B is depicted as the ratio of LC3-II over LC3-I after normalization against β-actin. Chloroquine was used as a positive control. Dotted line shows baseline of untreated conditions. Data represent the means ± SD from 2 individual experiments. *Abbreviations:* CQ = chloroquine; GR = gemcitabine resistant; PR = paclitaxel resistant; WT = wild type.

form autolysosomes.[30-32] However, comparison of LC3 and p62 protein levels at 6, 24, and 72 hours post-RT with the untreated controls revealed a differential response among the PDAC cell lines (Fig. 4B-D).

Regardless of their chemoresistant status, WT, GR, and PR PATU-T cells demonstrated an elevated LC3-II/I ratio upon radiation between 6 and 24 hours that returned to baseline 72 hours post-RT (Fig. 4B). In contrast, analysis using chloroquine, a compound used to inhibit the fusion of autophagosomes with lysosomes,[33] showed that autophagic flux was blocked in both PANC-1 and SUIT2-007 cell lines as evidenced by the accumulation of both LC3-I and II as well as p62 (Fig. 4C, D). Upon radiation, the LC3II/I ratio was similar to that of untreated PANC-1 and SUIT2-007 cells after 6 and 24 hours, respectively, and p62 expression decreased at 6 hours post-RT before basal expression of p62 returned at 24 hours post-RT. Collectively, these findings indicate that autophagy is induced in PANC-1 and SUIT2-007 cells upon irradiation.

Hippo signaling pathway

Next, we conducted a comprehensive investigation into potential alternative pathways regulated by MST4. To do so, we used the Search Tool for the Retrieval of Interacting Genes/Proteins (STRING) online database, employing a threshold of 50 interacting proteins in the first shell. The resulting analysis revealed that among the KEGG pathways, the Hippo signaling pathway exhibited the highest number of interactors, as indicated in Table 2 (9 out of 153 with a false discovery rate of 1.09e-^{07}). The Hippo signaling pathway is known to govern various cellular processes, including the control of cell growth and apoptosis, and has been implicated in chemoradioresistance in different cancer types,[9] although its involvement in PDAC has not been reported thus far. We proceeded by examining the modulation of protein expression of the core components (MST1/2, SAV1, LATS1, MOB1, and YAP/TAZ) at 6, 24, and 72 hours post-RT (Fig. E6). Interestingly, at 72 hours after irradiation, a major switch in the Hippo pathway to the "off" state was observed, with downregulation of MST1/2, SAV1, pMOB1, and phosphorylated YAP (pYAP) (S127 and S397) in SUIT2-007 cells (Figs. 5A, C and E7B) and of MST2, MOB1, and pYAP (S127 and S397) in PATU-T cells (Figs. 5A, B and E7A). When the pathway is in the "off" state, the phosphorylation of YAP decreases, triggering its nuclear translocation and target gene transcription along with other transcription factors, such as the transcriptional enhanced associate domain (TEAD) family members. To confirm increased nuclear translocation of YAP upon irradiation, its subcellular localization was determined by immunofluorescence (Fig. 5D). Compared with untreated controls, irradiated cells showed a higher YAP nucleus-to-cytosol ratio in SUIT2-007 cells, whereas statistical significance was not reached in the ratio in GR PATU-T cells (P = .6173). A trend toward increased nuclear translocation was also observed in PR PATU-T cells (P = .0791; Fig. 5E).

Table 2 KEGG pathways interacting with MST4 according to the STRING database

Pathway ID	Pathway description	Count in network	False discovery rate
hsa04390	Hippo signaling pathway	9 of 153	1.09 e-07
hsa04152	AMPK signaling pathway	8 of 120	2.23 e-07
hsa05160	Hepatitis C	8 of 156	1.06 e-06
hsa04114	Oocyte meiosis	7 of 120	3.10 e-06
hsa04530	Tight junction	7 of 156	1.38 e-05
hsa04151	PI3K-Akt signaling pathway	7 of 350	0.002
hsa04150	mTOR signaling pathway	5 of 151	0.005
hsa04392	Hippo signaling pathway	4 of 99	0.0055
hsa05142	Chagas disease	4 of 130	0.0136
hsa04140	Autophagy (animal)	4 of 159	0.0237
hsa04730	Long-term depression	4 of 182	0.0357
hsa05161	Hepatitis B	4 of 196	0.0432
hsa05203	Viral carcinogenesis	4 of 209	0.0448
hsa03015	mRNA surveillance pathway	3 of 27	0.027
hsa04350	TGF-beta signaling pathway	3 of 59	0.0172
hsa05205	Proteoglycans in cancer	3 of 91	0.0432
hsa04810	Regulation of actin cytoskeleton	3 of 93	0.0432

Abbreviation: STRING = Search Tool for the Retrieval of Interacting Genes/Proteins.

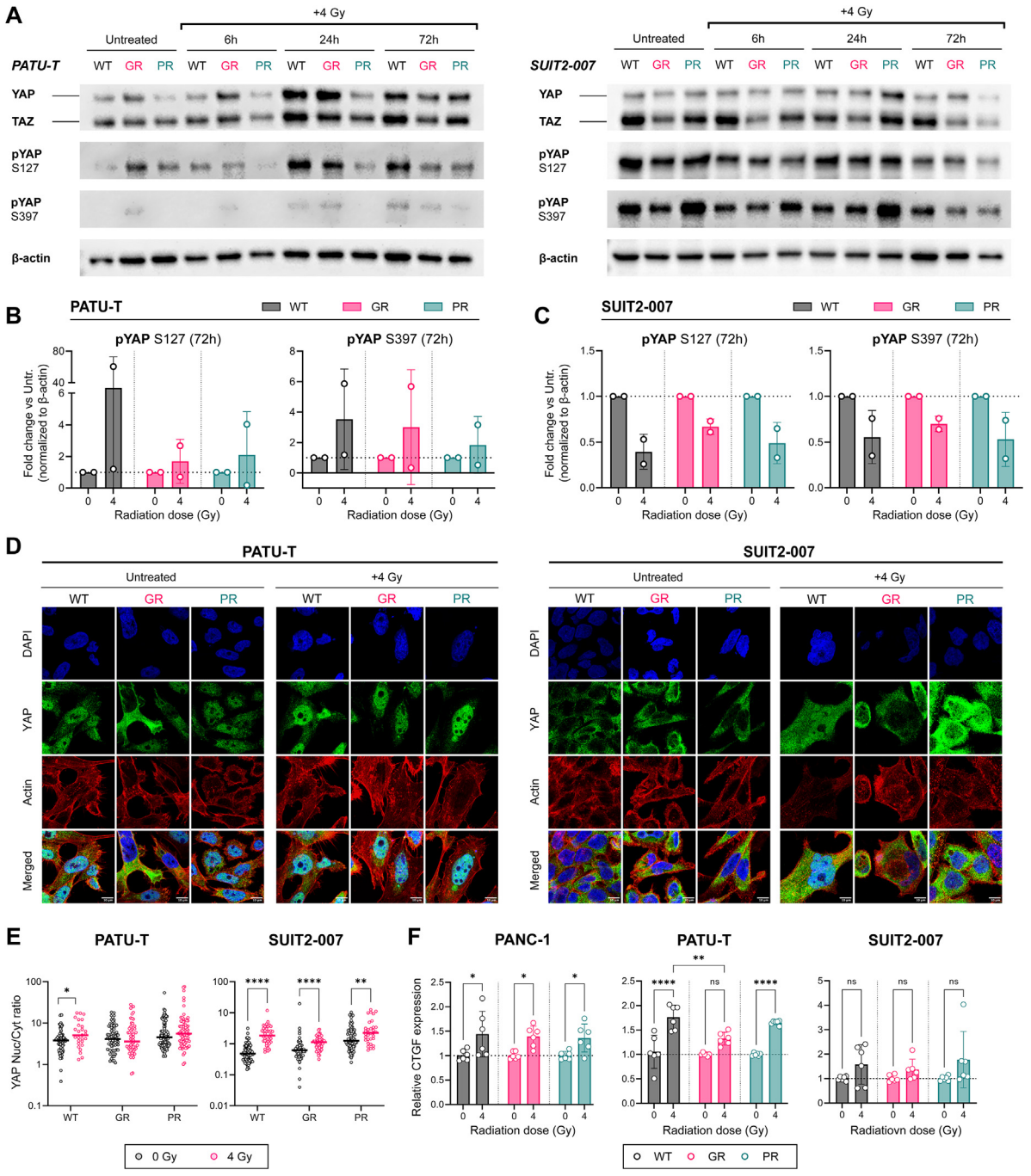

Fig. 5. The Hippo signaling pathway is modulated in response to radiation in pancreatic ductal adenocarcinoma. (A) Protein expression of total yes-associated protein (YAP) and its phosphorylation sites S127 and S397 were determined using Westen blot at 6, 24 and 72 hours after 4 Gy of radiation in PATU-T and SUIT2-007 cells. Beta-actin bands correspond to pYAP S397. Relative signal intensity of pYAP S127 and pYAP S397 expressions in (B) PATU-T and (C) SUIT2-007 cells at 72 hours after radiation. (D) Representative images of YAP staining (green) with actin staining for the cytoskeleton (red) and DAPI staining for the nucleus (blue) in untreated and irradiated pancreatic ductal adenocarcinoma cells. (E) Nuclear translocation of YAP as a measure of the Hippo pathway in the "off" state evaluated as a ratio of nuclear over cytosolic YAP at 72 hours after radiation. (F) *CTGF* levels in PANC-1, PATU-T, and SUIT2-007 cells measured with reverse-transcription quantitative polymerase chain reaction . Data represent the means ± SD from 2 individual experiments. *$P < .05$, **$P < .01$, ***$P < .001$, ****$P < .0001$. *Abbreviations:* GR = gemcitabine resistant; PR = paclitaxel resistant; pYAP = phosphorylated yes-associated protein; WT = wild type; YAP = yes-associated protein.

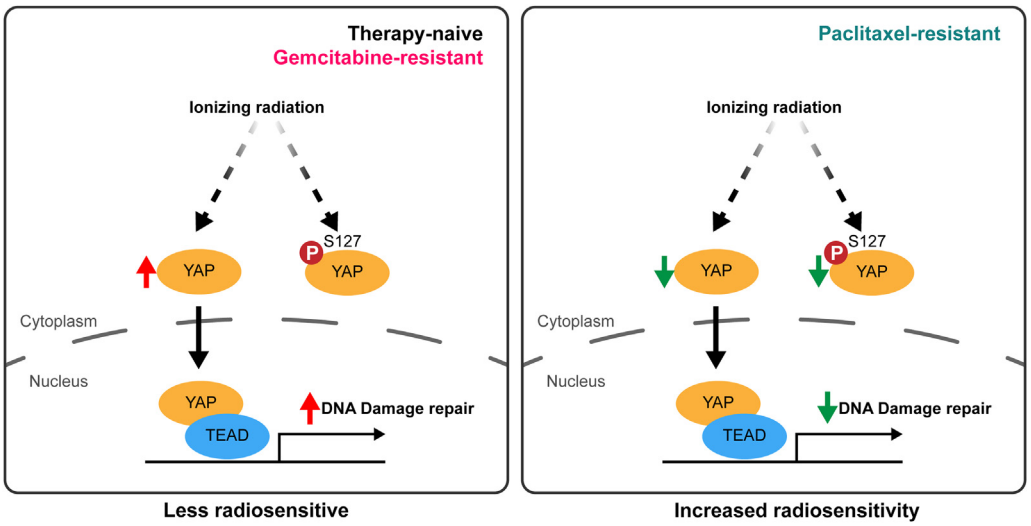

Fig. 6. Proposed underlying mechanism for the increased response to radiation in paclitaxel-resistant pancreatic ductal adenocarcinoma. In therapy-naïve and gemcitabine-resistant cells, total YAP expression is increased upon radiation, leading to increased DNA damage repair. In irradiated paclitaxel-resistant pancreatic ductal adenocarcinoma cells, total YAP expression and phosphorylated YAP (S127) expression is decreased, resulting in decreased DNA double-strand break repair. *Abbreviations:* TEAD = transcriptional enhanced associate domain; YAP = yes-associated protein.

To confirm the activation of the Hippo pathway upon irradiation, the expression of its bona fide target gene *CTGF* was measured by reverse-transcription quantitative PCR. In all PANC-1 and PATU-T cells, the *CTGF* mRNA level was significantly increased after irradiation. Although a trend toward increased *CTGF* expression was observed in SUIT2-007 cells (Fig. 5F), statistical significance was not reached. Considered together, these results indicate that the Hippo signaling pathway is involved in response to radiation in PDAC cells.

Discussion

This study is the first exploration of the effect of IR on acquired chemoresistance in PDAC cells. Our findings demonstrate that cells with acquired paclitaxel resistance manifest the highest susceptibility to IR as a result of increased apoptosis, DNA damage accumulation, and ROS production. Furthermore, depending on the unique cellular situation, radiation-induced modulation of autophagy and the Hippo pathway emerged as plausible underlying mechanisms, offering promising insights for tailoring personalized treatment strategies in patients with acquired chemoresistance.

As PDAC is an inherently therapy-resistant cancer, investigations of alternative treatments for it are ongoing. The currently available combined chemotherapy regimens, gemcitabine with (nab-)paclitaxel or FOLFIRINOX, only partially improve patient outcomes, with an increase in median OS favoring FOLFIRINOX over gemcitabine/nab-paclitaxel by only 2 months in the metastatic setting.[34]

Inevitably, patients progress despite polychemotherapeutic regimens, indicative of developing therapy resistance. As a result, extensive research into new targets and drug combinations to overcome PDAC chemoresistance, mainly into gemcitabine, is being conducted.[35-37] However, to date no new therapeutic option has been proven to increase patient survival, leaving an unmet need for patients with PDAC.[38] Prior studies reported that models made resistant to a specific drug could exhibit cross-resistance to other drugs[39,40] but also, most interestingly, increase sensitivity to other treatments, such as hyperthermia, in different human cancer cell lines.[41] Research into the differential responses to IR we found in our chemoresistant models could serve as a platform for exploring potential radiosensitivity and resistance in other chemoresistant models and how to overcome it.

Recent clinical trials reported promising results for RT in PDAC. A phase 1 trial evaluated concurrent gemcitabine/nab-paclitaxel with MRI-guided radiation in borderline resectable and locally advanced PDAC.[42] Another phase 1 study reported the safety of nab-paclitaxel chemotherapy induction followed by chemoradiation treatment.[43] Although the cohort was small and a control arm was not used, this study also suggested a favorable median survival compared with previous studies. Finally, the phase 3 PREOPANC-1 trial demonstrated superior 5-year OS for neoadjuvant chemoradiation (20.5%) compared with upfront surgery (6.5%).[6]

Despite these findings, whether and how acquired chemoresistance affects radiosensitivity in PDAC is still unclear and is being investigated. Previous in vitro studies focused on acquired radioresistance,[44,45] yet upfront RT is not often chosen in the clinical setting, with chemotherapy followed by RT usually preferred. For these reasons, we adopted an alternative approach, examining whether PDAC cells with acquired chemoresistance showed differential radiosensitivity and investigating the possible molecular mechanisms. Our collective findings show that PR PDAC cells were more

sensitive to IR than their parental counterparts, as evidenced by a relative increase in DNA damage, induction of early and late apoptosis, and decreased cell growth. As possible molecular mechanisms, we investigated autophagy and Hippo signaling, 2 pathways involved in IR response, and found that they are involved in differential response to IR in PDAC, although to a different extent in the different chemoresistant models. IR of PR cells resulted in an increase in accumulation of DNA damage and generation of ROS despite similar DNA damage repair induction as WT and as shown by γH2AX expression 24 hours post-RT.

It is important to note that we did not evaluate the nature and cause of the increase in accumulated DNA damage in our PR models. Specifically, the dichloro-dihydro-fluorescein diacetate assay employed in our study is limited to the general recognition of ROS and cannot identify the specific free radicals involved (eg, superoxide and hydroxyl radicals). The implications of the overall increase in ROS generation after radiation in these PR cells also remains unanswered. Of note, an increase in basal ROS generation and oxygen consumption rate has been reported in ROS generation of PR lung cancer models.[46] An enhanced generation of ROS might increase oxidative DNA damage and impair DNA damage recovery. Further studies on radiation-induced DNA injury and potential correlations with oxidative stress in PR models are therefore warranted.

Paclitaxel is a well-known radiosensitizer for many cancers, as cell arrest in the G2/M cell cycle phase augments radiation efficacy.[47] However, studies of paclitaxel-induced arrest in the G2/M phase have shown contradictory results and have reported it insufficient for radiosensitization of PDAC cells.[48] For these reasons, cells were not treated with paclitaxel for any experiments in our study, and we focused on the possible role of acquired stable chemoresistance. We assessed autophagy and Hippo signaling, 2 pathways involved in radiation response. In particular, macroautophagy is a dynamic multistep cellular process involved in regulating environmental stress cues and consequently in providing energy and other building blocks upon degradation of proteins and organelles.[49,50] Autophagy in cancer has been implicated to have a role in support of tumor growth and therapy resistance.[51] It has been reported that autophagy in PDAC is triggered upon irradiation[52] and that inhibition of autophagy in PDAC could sensitize cells to radiation.[53]

In our PR PDAC models, we found cell line−dependent activation of autophagy upon irradiation. A significant distinction among our PDAC models could be observed in *DPC4/SMAD4* status, as PANC-1 and SUIT2-007 cells express WT *SMAD4,* whereas *SMAD4* is deleted in PATU-T cells.[54,55] In vitro and clinical studies suggest that the loss of *SMAD4* in PDAC not only affects migratory potential but also leads to increased radioresistance through autophagy.[29,56,57] Thus, differences in *SMAD4* status could at least in part explain the discrepancies observed not only in activation of autophagy but also radiosensitivity. Keeping with these findings, silencing of *SMAD4* and mutations in *SMAD4* confer increased resistance to IR in other mesenchymal PDAC cell lines.[29] Although autophagy activation was not observed in PATU-T cells, it is plausible that the radiation dose may not have been sufficient to induce such response in these cells. However, in WT *SMAD4* PANC-1 and SUIT2-007 cells, autophagy was activated regardless of chemoresistant phenotype, and this activation coincided with the increased DNA damage accumulation found in our PR models.

The Hippo signaling pathway is a highly conserved signaling pathway that regulates cell growth and organ size whose dysregulation has been implicated in several cancers, including PDAC. Hippo signaling dysregulation in PDAC is relevant for tumor progression, recurrence, chemoresistance, and radiosensitivity.[58-60] Upon nuclear translocation of the key effector molecule, YAP acts as a cotranscriptional activator with various other transcriptional factors, such as TEAD family members, promoting transcription of genes involved in cell proliferation and survival but also radioresistance.[61,62] Remarkably, radiation also promotes nuclear translocation of YAP in mesenchymal cell lines PANC-1 and MIA PaCa-2, similar to our irradiated mesenchymal-like PATU-T and SUIT2-007 cell lines.[59] However, we observed variations between not only the 2 cell lines but also their chemoresistant clones, as evidenced by the time-dependent expression patterns of total YAP and pYAP.

Previous studies have emphasized the oncogenic potential of radiation-induced YAP activation, which leads to enhanced cell proliferation via distinct signaling pathways, such as the FGF2-MAPK and IGF2-Akt signaling pathways in glioblastoma multiforme and medulloblastoma, respectively,[61,62] whereas knockdown of YAP in endometrial cancer cells results in decreased proliferation.[63] Most recently, a study evaluating the association between TEAD protein and DNA damage repair proteins using immunoprecipitation analysis showed that TEAD proteins colocalize with DNA double-strand break repair proteins, such as RIF1, XRCC5, and XRCC6. Furthermore, silencing of TEAD proteins has been associated with a consistent decrease in cell survival upon treatment with radiation due to reduced DNA double-strand break repair via both nonhomologous end-joining or homologous recombination DNA repair pathways.[64]

In triple-negative breast cancer cells, disrupting the interaction between YAP and TEAD proteins with small molecule inhibitor verteporfin[65] has been shown to result in increased expression of DNA damage repair proteins.[10] Notably, increased γH2AX expression has been observed in silenced YAP or verteporfin-treated cells derived from mouse pancreatic adenocarcinoma. Moreover, YAP inhibition combined with radiation significantly has been shown to decrease tumor size in mice bearing pancreatic adenocarcinoma.[66] Therefore, the decrease in total YAP and pYAP expression observed in our study could be associated with diminished YAP binding to TEAD proteins and consequently reduced DNA damage repair and cell proliferation, explaining the differential radiosensitivity in our PR PDAC

models (Fig. 6). This hypothesis should prompt additional investigations to verify the involvement of YAP in interacting with TEAD proteins during DNA damage repair in chemoresistant models. Finally, translational studies in PDAC after chemotherapy-induced changes in radiosensitivity are further recommended.

Conclusion

In this study, we report enhanced radiosensitivity in PDAC models resistant to paclitaxel via increased DNA damage accumulation and ROS generation, resulting in increased apoptosis induction. Our collective data underscore that distinctive radiation-induced responses are mediated by by autophagy and YAP activation in a cell line−dependent context.

References

1. Siegel RL, Miller KD, Wagle NS, Jemal A. Cancer statistics, 2023. *CA: A Cancer J Clin* 2023;73:17-48.
2. Sung H, Ferlay J, Siegel RL, et al. Global cancer statistics 2020: GLOBOCAN estimates of incidence and mortality worldwide for 36 cancers in 185 countries. *CA A Cancer J Clin* 2021;71:209-249.
3. Halbrook CJ, Lyssiotis CA, Pasca Di Magliano M, Maitra A. Pancreatic cancer: Advances and challenges. *Cell* 2023;186:1729-1754.
4. Caparello C, Meijer LL, Garajova I, et al. FOLFIRINOX and translational studies: Towards personalized therapy in pancreatic cancer. *World J Gastroenterol* 2016;22:6987-7005.
5. Malla M, Fekrmandi F, Malik N, et al. The evolving role of radiation in pancreatic cancer. *Front Oncol* 2023;12 1060885.
6. Versteijne E, van Dam JL, Suker M, et al. Neoadjuvant chemoradiotherapy versus upfront surgery for resectable and borderline resectable pancreatic cancer: Long-term results of the Dutch randomized PREOPANC trial. *JCO* 2022;40:1220-1230.
7. Lomax ME, Folkes LK, O'Neill P. Biological consequences of radiation-induced DNA damage: Relevance to radiotherapy. *Clin Oncol* 2013;25:578-585.
8. Wu Y, Song Y, Wang R, Wang T. Molecular mechanisms of tumor resistance to radiotherapy. *Mol Cancer* 2023;22:96.
9. Xu X, Chen Y, Wang X, Mu X. Role of Hippo/YAP signaling in irradiation-induced glioma cell apoptosis. *CMAR* 2019;11:7577-7585.
10. Andrade D, Mehta M, Griffith J, et al. YAP1 inhibition radiosensitizes triple negative breast cancer cells by targeting the DNA damage response and cell survival pathways. *Oncotarget* 2017;8 98,495-98,508.
11. Hönscheid P, Datta K, Muders MH. Autophagy: Detection, regulation and its role in cancer and therapy response. *Int J Radiat Biol* 2014;90:628-635.
12. Ansari D, Ohlsson H, Althini C, et al. The Hippo signaling pathway in pancreatic cancer. *Anticancer Res* 2019;39:3317-3321.
13. La Verde G, Artiola V, Pugliese M, et al. Radiation therapy affects YAP expression and intracellular localization by modulating lamin A/C levels in breast cancer. *Front Bioeng Biotechnol* 2022;10 969004.
14. Li F, Peng X, Zheng L, et al. YAP nuclear translocation facilitates radiation resistance in nasopharyngeal carcinoma cells. *Biochem Biophys Res Commun* 2023;670:109-116.
15. Würdinger T, Badr C, Pike L, et al. A secreted luciferase for ex vivo monitoring of in vivo processes. *Nat Methods* 2008;5:171-173.
16. Bergonzini C, Gregori A, Hagens TMS, et al. ABCB1 overexpression through locus amplification represents an actionable target to combat paclitaxel resistance in pancreatic cancer cells. *J Exp Clin Cancer Res* 2024;43:4.
17. Che PP, Mapanao AK, Gregori A, et al. Biodegradable ultrasmall-in-nano architectures loaded with cisplatin prodrug in combination with ionizing radiation induces DNA damage and apoptosis in pancreatic ductal adenocarcinoma. *Cancers* 2022;14:3034.
18. Sciarrillo R, Wojtuszkiewicz A, Kooi IE, et al. Using RNA-sequencing to detect novel splice variants related to drug resistance in in vitro cancer models. *J Vis Exp* 2016;54714.
19. Vallés-Marti A, Mantini G, Manoukian P, et al. Phosphoproteomics guides effective low-dose drug combinations against pancreatic ductal adenocarcinoma. *Cell Rep* 2023;42:112581.
20. Ware MJ, Colbert K, Keshishian V, et al. Generation of homogenous three-dimensional pancreatic cancer cell spheroids using an improved hanging drop technique. *Tissue Eng Part C Methods* 2016;22:312-321.
21. Siebring-van Olst E, Vermeulen C, de Menezes RX, Howell M, Smit EF, van Beusechem VW. Affordable luciferase reporter assay for cell-based high-throughput screening. *J Biomol Screen* 2013;18:453-461.
22. Rovithi M, Avan A, Funel N, et al. Development of bioluminescent chick chorioallantoic membrane (CAM) models for primary pancreatic cancer cells: A platform for drug testing. *Sci Rep* 2017;7:44686.
23. Firuzi O, Che PP, El Hassouni B, et al. Role of c-MET inhibitors in overcoming drug resistance in spheroid models of primary human pancreatic cancer and stellate cells. *Cancers* 2019;11:638.
24. Kim H, Xue X. Detection of total reactive oxygen species in adherent cells by 2',7'-dichlorodihydrofluorescein diacetate staining. *J Vis Exp* 2020 Jun 23:(160):10.3791/60682.
25. Houweling M, Abdul UK, Brahm C, et al. Radio-sensitizing effect of MEK inhibition in glioblastoma in vitro and in vivo. *J Cancer Res Clin Oncol* 2023;149:297-305.
26. Avan A, Pacetti P, Reni M, et al. Prognostic factors in gemcitabine−cisplatin polychemotherapy regimens in pancreatic cancer: XPD-Lys751Gln polymorphism strikes back. *Int J Cancer* 2013;133:1016-1022.
27. Huang T, Kim CK, Alvarez AA, et al. MST4 phosphorylation of ATG4B regulates autophagic activity, tumorigenicity, and radioresistance in glioblastoma. *Cancer Cell* 2017;32:840-855.e8.
28. Slobodnyuk K, Radic N, Ivanova S, et al. Autophagy-induced senescence is regulated by p38α signaling. *Cell Death Dis* 2019;10:1-18.
29. Wang F, Xia X, Yang C, et al. SMAD4 gene mutation renders pancreatic cancer resistance to radiotherapy through promotion of autophagy. *Clin Cancer Res* 2018;24:3176-3185.
30. Yadav VK, Awasthi P, Behl R, Kumar A. HSc70 interactome reveal major role of macroautophagy and minor role of chaperone mediated autophagy in K-Ras G12V cell proliferation and survival. *J Proteomics* 2022;264 104614.
31. Mizushima N, Yoshimori T, Levine B. Methods in mammalian autophagy research. *Cell* 2010;140:313-326.
32. Yim WWY, Mizushima N. Lysosome biology in autophagy. *Cell Discov* 2020;6:6.
33. Mauthe M, Orhon I, Rocchi C, et al. Chloroquine inhibits autophagic flux by decreasing autophagosome-lysosome fusion. *Autophagy* 2018;14:1435-1455.
34. Chun JW, Lee SH, Kim JS, et al. Comparison between FOLFIRINOX and gemcitabine plus nab-paclitaxel including sequential treatment for metastatic pancreatic cancer: A propensity score matching approach. *BMC Cancer* 2021;21:537.
35. Cai B, An Y, Lv N, et al. miRNA-181b increases the sensitivity of pancreatic ductal adenocarcinoma cells to gemcitabine in vitro and in nude mice by targeting BCL-2. *Oncol Rep* 2013;29:1769-1776.
36. Chen R, Lai LA, Sullivan Y, et al. Disrupting glutamine metabolic pathways to sensitize gemcitabine-resistant pancreatic cancer. *Sci Rep* 2017;7:7950.
37. Ahmad IM, Dafferner AJ, O'Connell KA, et al. Heme oxygenase-1 inhibition potentiates the effects of nab-paclitaxel-gemcitabine and modulates the tumor microenvironment in pancreatic ductal adenocarcinoma. *Cancers* 2021;13:2264.
38. De Dosso S, Siebenhüner AR, Winder T, et al. Treatment landscape of metastatic pancreatic cancer. *Cancer Treat Rev* 2021;96 102180.

39. Aldonza MBD, Ku J, Hong JY, et al. Prior acquired resistance to paclitaxel relays diverse EGFR-targeted therapy persistence mechanisms. *Sci Adv* 2020;6:eaav7416.
40. Van Bree C, Kreder NC, Loves WJP, Franken NAP, Peters GJ, Haveman J. Sensitivity to ionizing radiation and chemotherapeutic agents in gemcitabine-resistant human tumor cell lines. *Int J Radiat Oncol Biol Phys* 2002;54:237-244.
41. Li Y, Zeng Y, Mooney SM, et al. Resistance to paclitaxel increases the sensitivity to other microenvironmental stresses in prostate cancer cells. *J Cell Biochem* 2011;112:2125-2137.
42. Kim H, Olsen JR, Green OL, et al. MR-guided radiation therapy with concurrent gemcitabine/nab-paclitaxel chemotherapy in inoperable pancreatic cancer: A TITE-CRM phase I trial. *Int J Radiat Oncol Biol Phys* 2023;115:214-223.
43. Koay EJ, Zaid M, Aliru M, et al. Nab-paclitaxel, capecitabine, and radiation therapy after induction chemotherapy in treating patients with locally advanced and borderline resectable pancreatic cancer: Phase 1 trial and imaging-based biomarker validation. *Int J Radiat Oncol Biol Phys* 2022;114:444-453.
44. Zuniga O, Byrum S, Wolfe AR. Discovery of the inhibitor of DNA binding 1 as a novel marker for radioresistance in pancreatic cancer using genome-wide RNA-seq. *Cancer Drug Resist* 2022;5:926-938.
45. Görte J, Danen E, Cordes N. Therapy-naive and radioresistant 3-dimensional pancreatic cancer cell cultures are effectively radiosensitized by β1 integrin targeting. *Int J Radiat Oncol Biol Phys* 2022;112:487-498.
46. Datta S, Choudhury D, Das A, et al. Paclitaxel resistance development is associated with biphasic changes in reactive oxygen species, mitochondrial membrane potential and autophagy with elevated energy production capacity in lung cancer cells: A chronological study. *Tumour Biol* 2017;39 1010428317694314.
47. Barbuti AM, Chen ZS. Paclitaxel through the ages of anticancer therapy: Exploring its role in chemoresistance and radiation therapy. *Cancers* 2015;7:2360-2371.
48. Liebmann JE, Fisher J, Teague D, Cook JA. Sequence dependence of paclitaxel (Taxol) combined with cisplatin or alkylators in human cancer cells. *Oncol Res* 1994;6:25-31.
49. Mulcahy Levy JM, Thorburn A. Autophagy in cancer: Moving from understanding mechanism to improving therapy responses in patients. *Cell Death Differ* 2020;27:843-857.
50. Debnath J, Gammoh N, Ryan KM. Autophagy and autophagy-related pathways in cancer. *Nat Rev Mol Cell Biol* 2023;24:560-575.
51. Yang S, Wang X, Contino G, et al. Pancreatic cancers require autophagy for tumor growth. *Genes Dev* 2011;25:717-729.
52. Suzuki M, Anko M, Ohara M, Matsumoto KI, Hasegawa S. Radiation-induced autophagy in human pancreatic cancer cells is critically dependent on G2 checkpoint activation: A mechanism of radioresistance in pancreatic cancer. *Int J Radiat Oncol Biol Phys* 2021;111:260-271.
53. Yazal T, Bailleul J, Ruan Y, et al. Radiosensitizing pancreatic cancer via effective autophagy inhibition. *Mol Cancer Ther* 2022;21:79-88.
54. Moore PS, Sipos B, Orlandini S, et al. Genetic profile of 22 pancreatic carcinoma cell lines. *Virchows Arch* 2001;439:798-802.
55. Bartsch D, Barth P, Bastian D, et al. Higher frequency of DPC4/Smad4 alterations in pancreatic cancer cell lines than in primary pancreatic adenocarcinomas. *Cancer Lett* 1999;139:43-49.
56. Fei N, Wen S, Ramanathan R, et al. SMAD4 loss is associated with response to neoadjuvant chemotherapy plus hydroxychloroquine in patients with pancreatic adenocarcinoma. *Clin Transl Sci* 2021;14:1822-1829.
57. Chen YW, Hsiao PJ, Weng CC, et al. SMAD4 loss triggers the phenotypic changes of pancreatic ductal adenocarcinoma cells. *BMC Cancer* 2014;14:181.
58. Hayashi H, Uemura N, Zhao L, et al. Biological significance of YAP/TAZ in pancreatic ductal adenocarcinoma. *Front Oncol* 2021;11 700315.
59. Gopal U, Mowery Y, Young K, Pizzo SV. Targeting cell surface GRP78 enhances pancreatic cancer radiosensitivity through YAP/TAZ protein signaling. *J Biol Chem* 2019;294 13,939-13,952.
60. Kapoor A, Yao W, Ying H, et al. Yap1 activation enables bypass of oncogenic Kras addiction in pancreatic cancer. *Cell* 2014;158:185-197.
61. Zhang Y, Wang Y, Zhou D, et al. Radiation-induced YAP activation confers glioma radioresistance via promoting FGF2 transcription and DNA damage repair. *Oncogene* 2021;40:4580-4591.
62. Fernandez-L A, Squatrito M, Northcott P, et al. Oncogenic YAP promotes radioresistance and genomic instability in medulloblastoma through IGF2-mediated Akt activation. *Oncogene* 2012;31:1923-1937.
63. Tsujiura M, Mazack V, Sudol M, et al. Yes-associated protein (YAP) modulates oncogenic features and radiation sensitivity in endometrial cancer. *PLoS One* 2014;9 e100974.
64. Calses PC, Pham VC, Guarnaccia AD, et al. TEAD proteins associate with DNA repair proteins to facilitate cellular recovery from DNA damage. *Mol Cell Proteomics* 2023;22 100496.
65. Liu-Chittenden Y, Huang B, Shim JS, et al. Genetic and pharmacological disruption of the TEAD−YAP complex suppresses the oncogenic activity of YAP. *Genes Dev* 2012;26:1300-1305.
66. Zhuang Y, Wang Y, Liu C, Li S, Du S, Li G. Yes-associated protein 1 inhibition induces immunogenic cell death and synergizes with radiation and PD-1 blockade. *Int J Radiat Oncol Biol Phys* 2023;116:894-905.